УДК 004.4

Yüksel Köseoğlu

(Suleyman Demirel University)

MAGNETIC PROPERTIES OF $NI_{0.5}ZN_{0.4}CU_{0.1}FE_2O_4$ NANO-COMPOSITE

(Представлена член-корреспондентом НАН РК Б.Ш.Кульпешовым)

Abstract

Magnetic properties of $Ni_{0.5}Zn_{0.4}Cu_{0.1}Fe_2O_4$ spinel ferrite prepared by co-precipitation technique have been investigated by VSM and electron spin resonance (ESR) technique at X-band in the temperature range of 30-300 K. The structural and morphological characterization of the sample was done by XRD and SEM. The size of the nanoparticles was found as 30 nm. VSM measurements have shown that the sample has superparamagnetic behavior at room temperature. It is seen that the line width, resonance field and intensity of the ESR signals are strongly temperature dependent. As the temperature is decreased, the line width is increasing while the resonance field is decreasing. The increse in the line width and the decrease in the resonance field can be attributed to the frozen surface spin profile giving rise to unidirectional anisotropy. Also at low temperatures, the disorder of the dipolar fields is increasing and antiferromagnetic interactions dominates and cause to spin disorder of the sample. Hence the magnetic anisotropy field increases.

Keywords: Magnetic properties, spinel ferrite, co-precipitation, technique have been investigated.

Ключевые слова: магнитные свойства, феррит-шпинели, осадочные, техника, исследования.

Тірек сөздер: тұнба техника, дайындау, шпинель-феррит, магниттік қасиет, зерттеу.

1. Introduction

Microwave absorption materials important to suppress microwaves reflected from metal structures inn both civil and stealth defence system for military platforms. The microwave absorbing characteristics, such as matching frequency, matching thickness and bandwidth should be considered to design the proper absorber. The absorption or dispersion of the electromagnetic energy in the medium, i.e., between the radar and a protected target by the use of radar absorbing materials to cover the metallic surface, is one of the methods of reducing the radar signature of the targets. The magnetic and dielectric properties such as permeability (μ), permittivity (ε) and loss constant (tan δ) have to be controlled due to its dependency on the absorbing characteristics. Since the complex ε of the ferrite absorber show rather constant values in the

GHz ranges, the microwave absorbing character tics strongly depending on the resonance phenomena of the ferrite body. A proper combination of complex permeability and permittivity is necessary to fabricate the zero-reflection microwave absorber with an impedance matching. Increasing of dielectric permittivity and development of an impedance matching is important in ferrite-polymer composite by adding of conducting materials.

Therefore in this work, we report on the vibrating sample magnetometry and electron spin resonance (ESR) investigations of magnetic properties of $Ni_{0.5}Zn_{0.4}Cu_{0.1}Fe_2O_4$ composite sample prepared by standart ceramic technique. The VSM and ESR measurements have been done in the wide range of temperatures, 30-300K.

2. Experimental

The complex ferrite system is composed of Zn^{2+}, Cu^{2+}, Ni^{2+} metal ions and has the formula of $Ni_{0.5}Zn_{0.4}Cu_{0.1}Fe_2O_4$. Thermodynamic modeling of the complex system shows that all the species required for the formation of the system are present in the form of oxide or hydroxide at a wide pH range of 7-14. Therefore, it is possible to obtain the complex ferrite phase by using the coprecipitation in that pH range. X-ray powder diffraction was used to determine the crystalline phases, and the effect of the heat treatment on the crystallinity and the crystal growth.

The $Ni_{0.5}Zn_{0.4}Cu_{0.1}Fe_2O_4$ solution was transferred into the 3 neck flask with water cooled condenser, temperature controller and N_2 gas flowing. The silanization was performed 24 hrs at 80 °C under vigorous stirring. APTMS acts as a coupling agent, where silanization takes place on the particle surfaces bearing hydroxyl groups in the organic solvent. This results in the formation of a three-dimensional polysiloxane networks. The silanized $Ni_{0.5}Zn_{0.4}Cu_{0.1}Fe_2O_4$ samples were cooled down to the room temperature and the supernatant was removed form the precipitation by decantation. The precipitated powder was dried in vacuum over at 120 °C for 2 hrs. Composite specimens of $Ni_{0.5}Zn_{0.4}Cu_{0.1}Fe_2O_4$ a with a 5 pbw of graphite powder was dispersed in PMMA. 50 mL MMA, 0.5wt% AIBN and 200 μL acetic acid were mixed with vigorous magnetic stirring and heated at 80 °C with reflux. After 10 min later, the hot plate was stopped and cooled down to room temperature. Rather viscous polymerized PMMA solution was formed. Another 25 ml MMA solution was prepared with silanized $Ni_{0.5}Zn_{0.4}Cu_{0.1}Fe_2O_4$ mixtures by adding the weight ratio of Pluronic® F87 NF to nanopowder was 0.1. After the mixture was sonicated for 10 min in water-cooled bath, the viscous pre-polymerized PMMA solution was added into the mixture of 25 mL MMA/nanopowder/surfactant and sonicated 5 min in water cooled bath. The mixture was transfer into clean 3-neck flask again and reheated at 80 °C with reflux. After 10 min later, the hot plate was cooled down to the room temperature and sonicated for 10 min in water-cooled bath. The final solution was transferred into screw capped glass container with a diameter 20 cm and tightly closed. The container was placed in silicon oil bath and kept 70 °C for 48 hrs. After open the cap of the container, the temperature was increased to 95 °C for 1 hr to evaporate the unreacted monomer.

For ESR measurements, the commercial X-band ($\nu \approx 9.7$ GHz) *Bruker EMX* model spectrometer was used. The sample was placed at the maximum magnetic field in the cavity. A cylindrical quartz tube was used to mount the sample in the cavity. The field derivative of microwave power absorption, dP/dH, was registered as a function of DC magnetic field H. To obtain the intensity of microwave power absorption, P, digital integration of the ESR curves was performed by using *Bruker WinEPR* software.

3. Results and Discussions

Structural and morphological characterization

From the Transmission Electron Microscopy (TEM) images of $Ni_{0.5}Zn_{0.4}Cu_{0.1}Fe_2O_4$ ferrite nanoparticles shown in Fig. 1 a and b, as-prepared particle shows rather irregular shapes comparing to the heat treated samples shows spherical shapes. Moreover, the TEM image of the heat-treated samples revealed darker region than as-prepared sample due to the crystallization. The average size of the particles is almost 30 nm. Regarding the peaks positions in Fig. 1c, the X-ray diffraction (XRD) pattern of $Ni_{0.5}Zn_{0.4}Cu_{0.1}Fe_2O_4$ corresponds well to reference patterns of $Ni_{0.5}Zn_{0.4}Cu_{0.1}Fe_2O_4$ spinel ferrites. This indicates that the spinel structure of $Ni_{0.5}Zn_{0.4}Cu_{0.1}Fe_2O_4$ has been successfully produced as a single phase by the controlled chemical co-precipitation method.

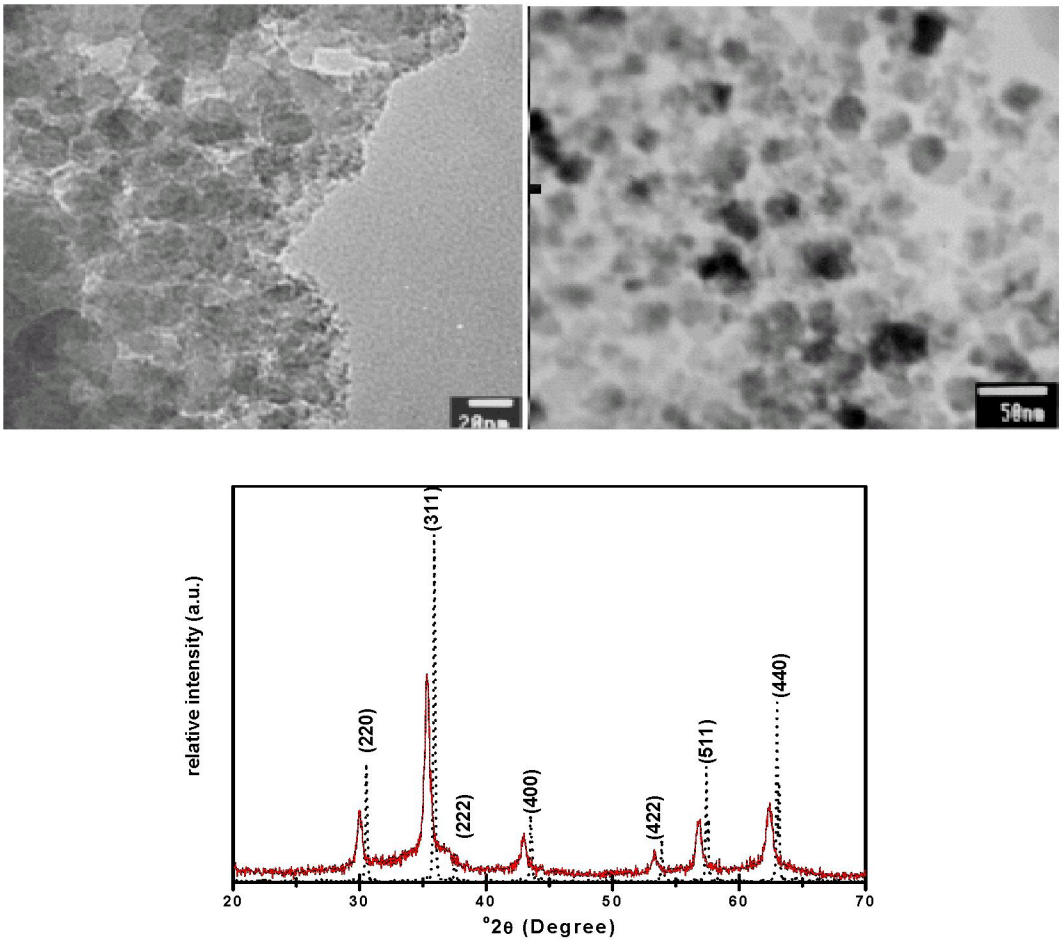

Figure 1: TEM images of $Ni_{0.5}Zn_{0.4}Cu_{0.1}Fe_2O_4$ ferrite nanoparticles (a) as-prepared, (b) heat treated at 450 °C for 2 hrs and (c) X-ray diffraction patterns

VSM results

Hysteresis loops of the ferrite composites, obtained by using a Quantum Design PPMS VSM magnetometer, are presented in figure 3 (a) for 300 K and (b) 50 K. The sample exhibits very small hysteretic behavior at room temperature with a rounded shape characteristic for superparamagnetic particles. While the saturation magnetization at room temperature is 6.5 emu/g, it reaches to a value of 14 emu/g at 50 K. At room temperature the sample does not show any coercivity but it has a coercivity of 170 Oe at lowest temperature.

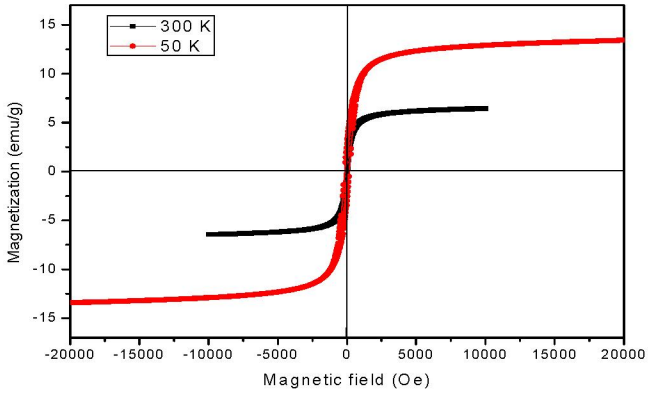

Figure 2: *M-H* loops of the sample measured at room temperature and 50 K

ESR results

In the present work the ESR spectra of polymeric complex ferrites were recorded as a function of temperature. The resonance field, line width and the signal intensity of the ESR signal were estimated in the temperature range of 10-300 K. The first derivative of the microwave power absorption (dP/dH, in arbitrary units) was recorded as a function of the applied field H in the range 0–7000 Oe. Experiments were performed at 9.5 GHz. The modulation field has a frequency of 100 kHz and amplitude of 15 Oe.

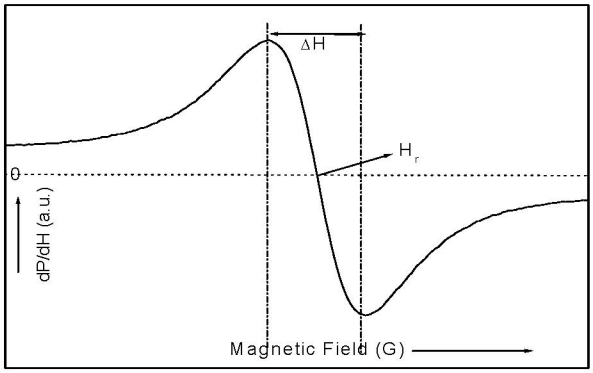

Figure 3: Analysis of ESR signal

The resonance field, H_r, measured from the magnetic field at the centre of the ESR resonance curve, and the distance between the bounding peaks of the first derivative of the absorption line defines the experimental width, □H, of the resonance, are shown in figure 1. The signal intensity was found by taking the second integral of the ESR signal.

The ESR spectra of polymeric complex ferrites of $Ni_{0.5}Zn_{0.4}Cu_{0.1}Fe_2O_4$ nanoparticles were recorded as a function of temperature. The derivative of microwave power absorbed by the sample with respect to the static magnetic field *dP/dH* is plotted as a function of static field for some selected temperatures as shown in Figure 4.

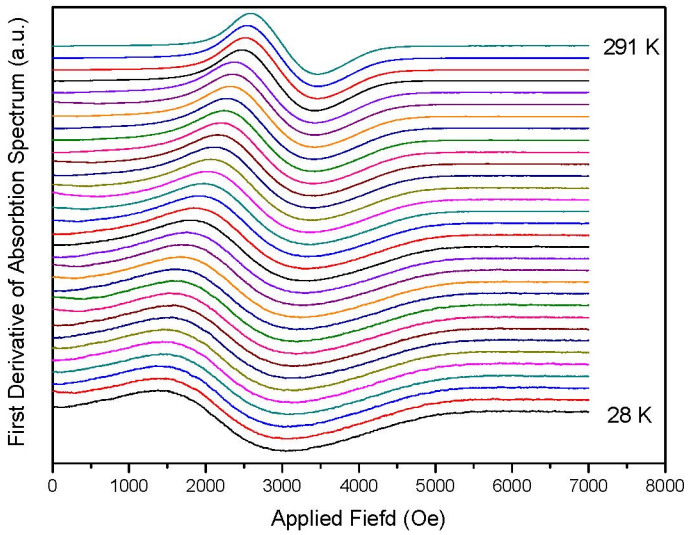

Figure 4: Some selected X-Band ESR spectra for $Ni_{0.5}Zn_{0.4}Cu_{0.1}Fe_2O_4$ samples.

As it is seen from this figure, the line width and the resonance field of the ESR spectra are strictly temperature dependent. At room temperature the values of the line width and the resonance field are 880

Oe and 3017 Oe, respectively. While the line width is increasing the resonance field is decreasing by the decrease in temperature.

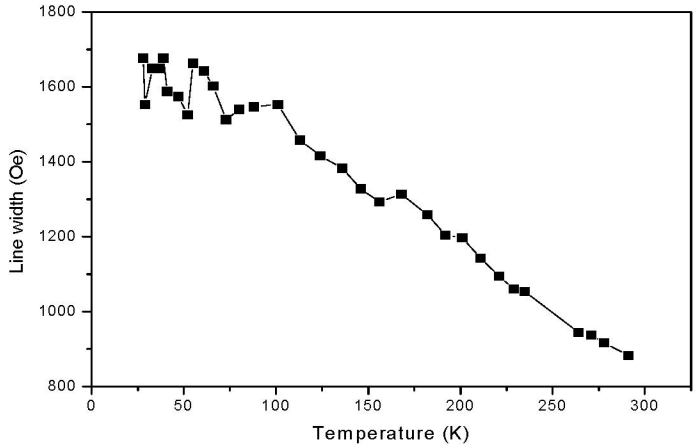

Figure 3: Temperature dependence of the ESR line width

Figure 3 shows the temperature variation of the line width values of the ESR spectra. As seen from the figure, the line width increases linearly as the temperature decreases down to lowest value. It is known that in a randomly oriented dispersed ferromagnet the absorption line width turns out to be a non-monotonic function of temperature. At low temperature the line width is large due to the scatter in direction of anisotropic field of the particles (inhomogeneous broadening). As the temperature increases the tendency to make magnetic moment isotropic causes the line width to decrease.

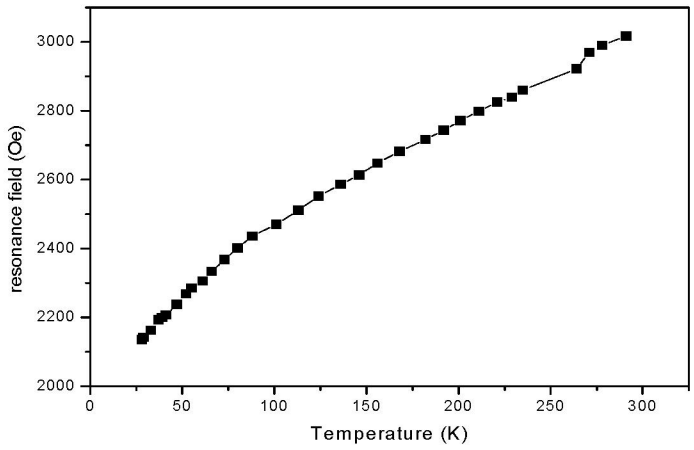

Figure 4: Temperature variation of the ESR resonance field.

Figure 4 indicates the variation of the resonance field values (measured from the magnetic field at the center of the ESR resonance curve) with the temperature. The figure implies that the resonance field decreases almost linearly when the temperature decreases down to lowest value opposite to the line width curve. It is known that dependence of uniaxial anisotropy energy on temperature is similar to that of magnetostatic i.e. demagnetisation energy [1]. Thus H_r will increase with temperature. This behaviour can be explained on the line similar to that suggested by Kodama et al. [13]. Below the blocking temperature, the surface spin freezes and they freeze in the direction of DC-magnetic field. This yield an exchange coupling between the surface and core spins. This gives rise to a 'unidirectional' anisotropy with easy axis in the direction of the field [1, 4]. As a result there is a decrease in the resonance field below blocking temperature. These results can easily be seen in fig.5 which represents the temperature variation of magnetic anisotropy field (obtained by H(room) - H(r); where H(room) is the resonance field at room temperature and H(r) is the resonance field at any temperature).

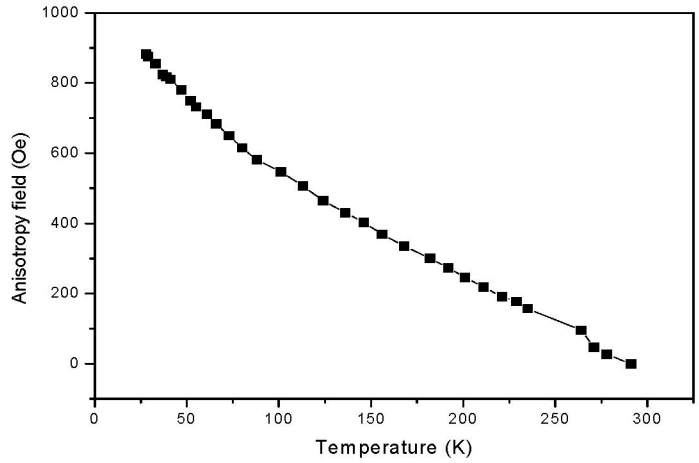

Figure 5: Anisotropy field vs. Temperature

It seen that while the temperature is decreasing anisotropy field is increasing. The reason for this, at low temperatures, the anisotropic energy KV is larger than the thermal energy k_BT to render the nanoparticles to be blocked readily. Also, the reduction of the magnetic domain size at low temperatures increases with the microwave power absorption [14]. At high temperatures, k_BT is greater than the energy barrier, only thermal energy is required to reorient the domains/particles and diminishing hysteresis is observed as expected in the superparamagnetic behavior. We remark the existence of two behaviors, one at high and the other at low temperature. In the high temperature regime we observed a superparamagnetic behavior. That means the effective anisotropy is small and thermal fluctuations governs the physics of the system. At low temperature the SPR behavior shows signs of a high anisotropy. Extrapolation to low-T of the high-T behavior evidences the effects of a large anisotropy developing at low-T. This anisotropy cannot be originated by the shape of the particle, so it can be expected to be originated on the particle surface and this agrees with the magnetization measurements and Monte-Carlo simulations performed on the nanoparticle system [15]. So, the results can be interpreted by a simple model, in which each single-domain nanoparticle is considered as a core-shell system, with uniaxial anisotropy on the core and surface anisotropy on the shell. The surface contribution is more evident in the absence of interparticle interactions [16, 17].

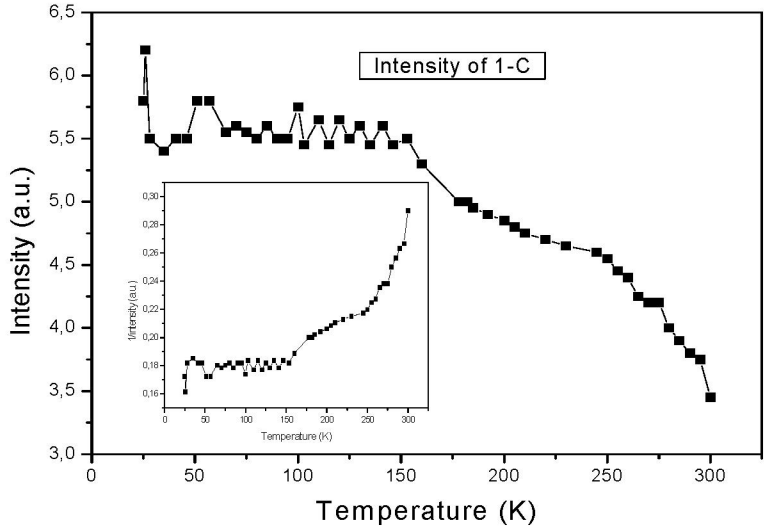

Figure 6: ESR signal intensity versus temperature

Figure 6 represents the temperature variation of ESR signal intensity (corresponding to dc susceptibility derived from magnetization) obtained from second integral of the ESR signals [5, 6]. The

inset shows the temperature dependence of inverse intensity. According to the figure, the signal intensity is increased slowly down to 150 K. Below this temperature; it approximately stabilizes between 150 and 60 K and seems almost constant. From this figure, one can see that the magnetization curve of this sample shows a maximum at around 60 K. The intensity of the ESR signals starts to increase below 60 K and then decrease down to 40 K. Below 40 K, it increases sharply by decreasing the temperature. Since the intensity curve is equivalent to dc susceptibility, this kind of behaviour of the signal intensity can be attributed to the spin glass nature of the sample, originating from antiferromagnetic interactions between the magnetic spins of the sample.

ESR experiments render information on the internal magnetic order of the nanoparticles. At high temperatures, the ESR line shape is governed by the core anisotropy and the thermal fluctuations. By decreasing temperature, as the shell spins increase their magnetic susceptibility, they produce an effective field on the core, leading to a decrease of resonance field from its high temperature value. As the shell spins begin to order the effective anisotropy increases following its surface value more closely.

As a result, the broadening of the line width and the decrease in the resonance field values by decreasing the temperature can be attributed to surface spin disorder (spin frustration) possibly coming from mainly antiferromagnetic interactions between the neighbouring spins in the magnetic grains. This frustration might be partially connected to dipolar interactions between the magnetic clusters. This can be related to the behaviour of the whole system as a solid with respect to magnetism and this disordered and frozen spin profile with respect to ESR, average effect is becoming important. Normally, the internal magnetic field originating from magnetic entities is expected to be more uniform as a result of highly ordered magnetic moments at low temperatures; giving narrower ESR line in contrary in our case. However, at low temperatures, one may expect the order of the system and a decrease in the inhomogenity of the dipolar fields. But, experimental results show the reverse of this (means at low temperatures the disorder of the dipolar fields is increasing, because the magnetization is not increasing with the same ratio), it can be said that some of the antiferromagnetic interactions are effective and this effect enhances the disorder of the system.

It should be noted that, in any ESR measurement, gyromagnetic (Larmour) precession frequency is observed in an effective field. Therefore, the shift in the resonance field value and the line width broadening are a clear indication to the induced fields (exchange anisotropy field), which is the main cause of the frustration (disorder) of any magnetic system. That is the increase in microscopic fields at low temperatures reveals itself as the line broadening and the decrease in the signal intensity.

These types of nanomaterials can be used in electronics and stealth technology as radar absorbing materials.

Резюме

Yüksel Köseoğlu

(Сүлеймен Демирел атындағы университет)

ТҰНБА ТЕХНИКАСЫМЕН ДАЙЫНДАЛҒАН $Ni_{0.5}Zn_{0.4}Cu_{0.1}Fe_2O_4$ МАГНИТТІК ҚАСИЕТТЕРІ

Тұнба техникасымен дайындалған $Ni_{0.5}Zn_{0.4}Cu_{0.1}Fe_2O_4$ шпинель ферритінің магниттік қасиеттері VSM және электрон айналу резонанс (ESR) техникасы арқылы X-диапазонында температура 30-300К аралығында зерттелді. Нұсқаның құрылымдық және морфологиялық сипаттамасы XRD мен SEM арқылы дайындалды. Нанобөлшектердің өлшемі 30нм екені табылды. VSM өлшеулері нұсқаның бөлме температурасында суперпарамагнетикалық қасиеттері бар екенін көрсетті. Түзудің қалыңдығы, резонанс өрісі және ESR сигналдарының қырқындылығы температураға өте тәуелді екені табылды. Температура азайған сайын түзу қалыңдайды, ал резонанс өрісі кішірейеді. Түзудің қалыңдауы және резонанс өрісінің азаюы бірбағыттық анизотропияны үлкейтетін қатырылған беттік спин профилі арқылы түсіндіріледі. Төмен температураларда биполярлы өрістің ретсіздігі өседі, антиферромагнетикалық әрекеттесулер үстем болады, бұл нұсқаның спин ретсіздігіне әкеледі. Демек, магниттік анизотроптық өріс өседі.

Тірек сөздер: шпинель ферриті, магниттік қасиет, резонанс өрісі, спин профилі, анизотроптық өріс.

Резюме

Yüksel Köseoğlu

(Университет им. Сулеймана Демиреля)

МАГНИТНЫЕ СВОЙСТВА НАНО-КОМПОЗИТОВ $Ni_{0.5}Zn_{0.4}Cu_{0.1}Fe_2O_4$

Магнитные свойства феррит-шпинели $Ni_{0.5}Zn_{0.4}Cu_{0.1}Fe_2O_4$, полученные осадочной техникой были исследованы с помощью VSM и техники электронно-вращательного резонанса (ESR) на диапазоне X при температуре в промежутке 30-300K. Структурная и морфологическая характеристика образца сделана с помощью XRD и SEM. Размер наночастиц составил 30нм. Измерения VSM показали, что образец обладал суперпарамагнетическими свойствами при комнатной температуре. Установлено, что толщина линии, резонансное поле и интенсивность сигналов ESR очень сильно зависят от температуры. По мере того как температура уменьшается, толщина линии увеличивается, а резонансное поле уменьшается. Увеличение толщины линии и уменьшение резонансного поля объясняется замороженным профилем поверхностного спина, повышающий однонаправленную анизотропию. При низких температурах растет беспорядок биполярных полей и доминируют антиферромагнетические взаимодействия, это в свою очередь приводит к спин беспорядку образца. Следовательно увеличивается магнетическое анизотропное поле.

Ключевые слова: феррит-шпинель, магнитное свойство, резонансное поле, профиль спина, анизотропное поле.

REFERENCES

1 Misbah-ul-Islam, K. A. Hashmi, M.U. Rana, T. Abbas, Solid State Communications 121 (2002) 51.

2 R.H. Kodama, A.E. Berkowitz, E.J. McNiff, Jr., S. Foner, J. Appl. Phys. 81 (1997) 5552.

3 R. Massart, D. Zins, F. Gendron, M. Rivoire, R.V. Mehta, R.V. Upadhyay, P.S. Goyal, V.K. Aswal, J. Magn. Magn. Mater. 201 (1999) 73.

4 Landolt-Börnstein, New Series III/4b, Springer, New York, 1970.

5 Horng-Tay Jeng, G.Y. Guo, J. Magn. Magn. Mater. 240 (2002) 436.

6Li Guang-She, Li Li-Ping, R.L. Smith Jr., H. Inomata, J. Mol. Struct. 560 (2001) 87.

7 M.H. Sousa, E. Hasmonay, J. Depeyrot, F.A. Tourinho, J. C. Bacri, E. Dubois, R. Perzynski, Yu. L. Raikher, J. Magn. Magn. Mater. 242-245 (2002) 572.

8 D. Zins, K. Nakatsuka, F. Gendron, M. Rivoire, J. Magn. Magn. Mater. 201 (1999) 84.

9 Y. Köseoğlu, R. Yilgin, J.V. Yakhmi, J. Qin, X. Chen, B. Aktaş, J. Magn. Magn. Mater. 258-259 (2003) 141.

10 Y. Köseoğlu, F. Yildiz, J.V. Yakhmi, J. Qin, X. Chen, B.Aktaş, J. Magn. Magn. Mater. 258-259 (2003) 416.

11 Y. Köseoğlu, O. Yalçın, F. Yıldız and B. Aktaş, J. Magn. Magn. Mater. 272-276 (2004) e1643.

12 Y. Köseoğlu, B. Aktaş, F. Yıldız, D.K. Kim, M. Toprak, M. Muhammed, Physica C 390/3 (2003) 197-203.

13 R.H. Kodama, J. Magn. Magn. Mater. 200 (1999) 359.

14 R. Berger, J. Bissey, J. Kliava, H. Daubric, C. Estournes, J. Magn. Magn. Mater. 234 (2001) 535.

15 R. Berger, J.C. Bissey and J. Kliava, J. Phys.: Condens. Matter 12 (2000) 9347.

16 R.D. Zysler, H. Romero, C.A. Ramos, E. De Biasi, D. Fiorani, J. Magn. Magn. Mater. 266 (2003) 233.

17 Y. Köseoğlu, H. Kavas, J. Nanosci.& Nanotechnol. 8 (2008) 584.

Поступила 22.11.2013 г.